Iranian Journal of Materials Forming 9 (1) (2022) 41-46

Online ISSN: 2383-0042

IJMF

Iranian Journal of Materials Forming

Journal Homepage: http://ijmf.shirazu.ac.ir

Research Article

Thermo-Mechanical Treatment of $AlCoCrFeNi_{2.1}$ High-Entropy Alloy

S.A. Erfani Mobarakeh* and K. Dehghani

Department of Materials and Metallurgical Engineering, Amirkabir University of Technology (Tehran Polytechnic), Hafez Ave., P.O. Box 15875-4413, Tehran, Iran

ARTICLE INFO

Article history:

Received 6 January 2022
Reviewed 7 February 2022
Revised 13 February 2022
Accepted 14 February 2022

Keywords:

Eutectic high-entropy alloy (EHEA)
Cold rolling
Annealing
Hardness
Shear punch test (SPT)

ABSTRACT

In this study, the microstructural evolutions, formed phases, micro- and macro-hardness changes and shear properties were evaluated in the as-cast, homogenized, cold-rolled and annealed $AlCoCrFeNi_{2.1}$ eutectic high-entropy alloy (EHEA). These studies were carried out using X-ray fluorescence (XRF), scanning electron microscopy (SEM), Rockwell C and Vickers hardness testing as well as shear punch testing (SPT). The microstructure after cold rolling followed by annealing was consisted of an elongated phases/grains in the direction of cold rolling and in almost equiaxed phases/grains. The homogenized specimen has the minimum amounts of hardness and yield/ultimate shear strength. Due to the presence of both elongated and equiaxed structures in the cold-rolled and annealed sample, the hardness and yield/ultimate shear strength of this specimen is between that of as-cast and homogenized cases.

1. Introduction

High-entropy alloys (HEAs) are multi-component systems composed of at least five main elements. These alloys offer extraordinary physical and mechanical properties such as high strength, corrosion resistance, abrasion resistance, and fatigue strength [1-4]. Single phase HEAs with FCC and BCC structures, have good ductility and high strength, respectively; therefore, achieving an optimum combination of strength and ductility in single phase HEAs is very difficult [5-9]. $AlCoCrFeNi_{2.1}$ is a eutectic high-entropy alloy (EHEA) with lamellar structure containing a combination of hard phase BCC and soft phase FCC providing both ductility and strength simultaneously [10-13].

Wani et al. [14] investigated the possibility of microstructural refinement and improvement of mechanical properties by severe cold-rolling in $AlCoCrFeNi_{2.1}$ lamellar high-entropy alloy. They found that severe cold-rolling and annealing can extremely improve the mechanical properties of $AlCoCrFeNi_{2.1}$ EHEA. Lozinko et al. [15] studied microstructural changes and mechanical properties during annealing at 800°C in a 90% cold-rolled $AlCoCrFeNi_{2.1}$ eutectic high-entropy alloy. They reported that the work-hardening capacity of each annealed sample is lower than that of the cold-rolled specimen.

In this study, after homogenization, cold rolling and subsequent annealing in high-entropy alloy $AlCoCrFeNi_{2.1}$, the effects of each process were

* Corresponding author
E-mail address: seyedalierfani@gmail.com (S.A. Erfani Mobarakeh)
https://doi.org/10.22099/IJMF.2022.42709.1210

evaluated on microstructural evolutions, hardness changes and shear properties of the alloy $AlCoCrFeNi_{2.1}$.

2. Materials and Methods

The $AlCoCrFeNi_{2.1}$ high-entropy alloy, was produced using vacuum arc remelting (VAR) furnace. The ingots (8 cm×3 cm×1.1 cm) were re-melted four times and then homogenized at 1100°C for 24 h to increase the homogeneity of alloying elements [16]. The chemical composition of the homogenized structure was measured through a Philips X Unique II XRF machine and the results are provided in Table 1.

Table 1. Chemical composition of the studied alloy (wt.%)

Alloy	Al	Co	Cr	Fe	Ni
$AlCoCrFeNi_{2.1}$	8.1	18.5	16.7	17.9	38.6

Homogenized specimens were then cut into 6 parts. The dimensions of each part/sample were 8 cm×3 cm×0.18 cm. Subsequently, the homogenized samples were subjected to annealing in the Muffle furnace at 950°C for 4 h after cold rolling with approximately a 17% reduction in thickness [17]. The cold rolling schedule is shown in Table 2.

Table 2. Cold rolling schedule

Pass No.	Initial thickness (mm)	Final thickness (mm)	Reduction in thickness (%)
1	1.8	1.725	4.16
2	1.725	1.65	4.34
3	1.65	1.575	4.54
4	1.575	1.5	4.76

The hardness of samples was measured by a Vickers hardness tester (Shimadzu brand, series M) with the load of 100 g and holding duration 10 s. Besides, macro-hardness of samples was measured by a Rockwell hardness tester in Rockwell C (HRC); The average of hardness was calculated from four measurements per each sample.

The shear properties of the samples were determined through conventional shear punch testing (SPT) using a flat punch with a 3 mm diameter by a universal Santam STM50 test machine at room temperature. In Fig. 1, the SPT apparatus and its schematic is demonstrated. The thickness of the samples was 0.4 mm. The test was performed at a constant crosshead speed of 0.3 mm/min [17, 18]. The stress-elongation curves were plotted using the recorded machine force-displacement data by utilizing the following equation [19]:

$$\tau = \frac{P}{2\pi r t} \quad (1)$$

where τ = shear stress, P = load, t = thickness of the specimen, and r = average of punch and lower die radius.

3. Results and Discussion

3.1. Microstructural evolutions

SEM micrograph of Fig. 2 represents the eutectic structure of as-cast $AlCoCrFeNi_{2.1}$ alloy, consisting of a

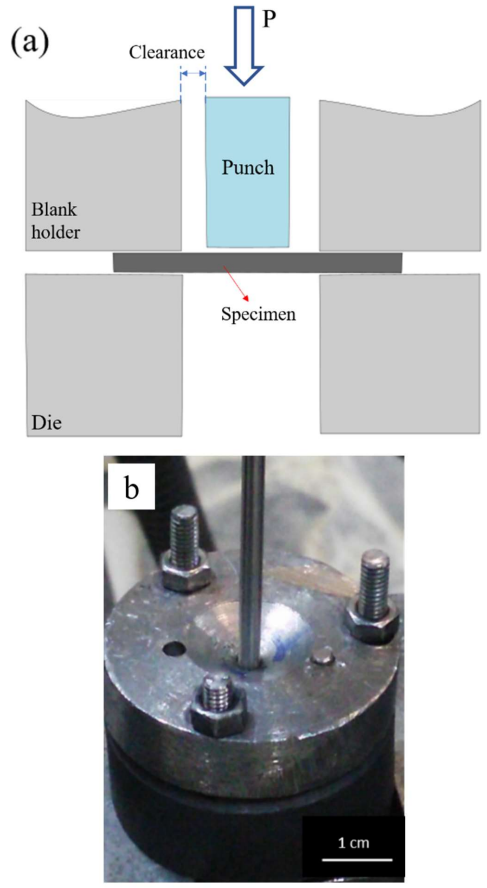

Fig. 1. (a) Schematic of the SPT; (b) SPT apparatus.

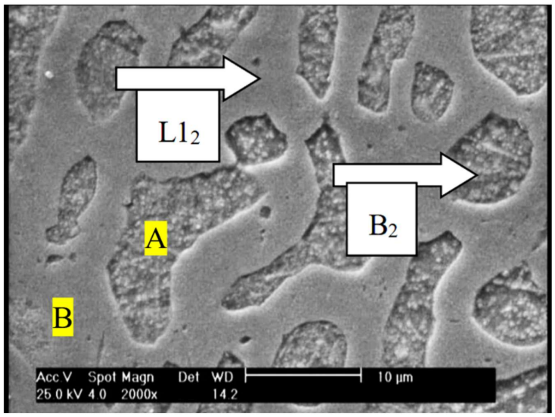

Fig. 2. SEM micrograph of the as-cast specimen with eutectic structure, consisting of L1$_2$ (FCC) phase and B$_2$ (BCC) phase.

FCC/L1$_2$ phase and the BCC/B$_2$ phase. In B$_2$ phase, some white Cr-rich precipitates are visible. These findings are reported based on the studies of Asoushe et al. [5], Gao et al. [20] and Wani et al. [21]. Figs. 3 and 4 show the EDS results of points "A" and "B" marked in Fig. 2, respectively. According to the EDS results, point "A" represents the NiAl-rich B$_2$ phase and point B belongs to the Cr-rich L1$_2$ phase.

According to Fig. 5 that indicated the microstructure of homogenized samples, the percentage of L1$_2$ phase has enhanced compared to the as-cast alloy. This is likely due to the diffusion of elements and dissolution of precipitates at high temperatures.

In the cold-rolled and annealed specimens, in some regions, the formed phases are elongated in the direction of the cold rolling; whereas in the other regions, the structure consists of equiaxed phases/grains (Fig. 6).

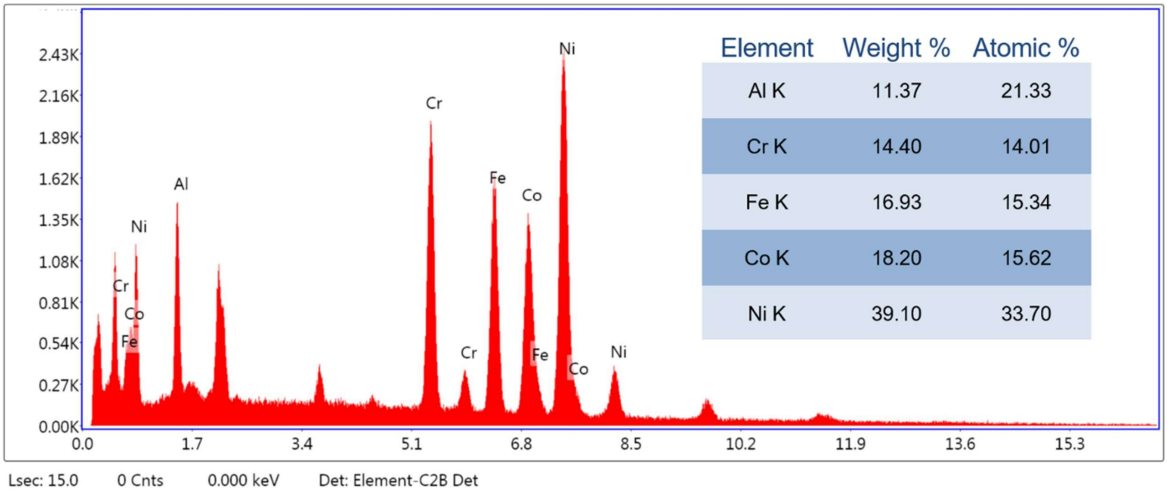

Element	Weight %	Atomic %
Al K	11.37	21.33
Cr K	14.40	14.01
Fe K	16.93	15.34
Co K	18.20	15.62
Ni K	39.10	33.70

Fig. 3. EDS results of point "A" in Fig. 2.

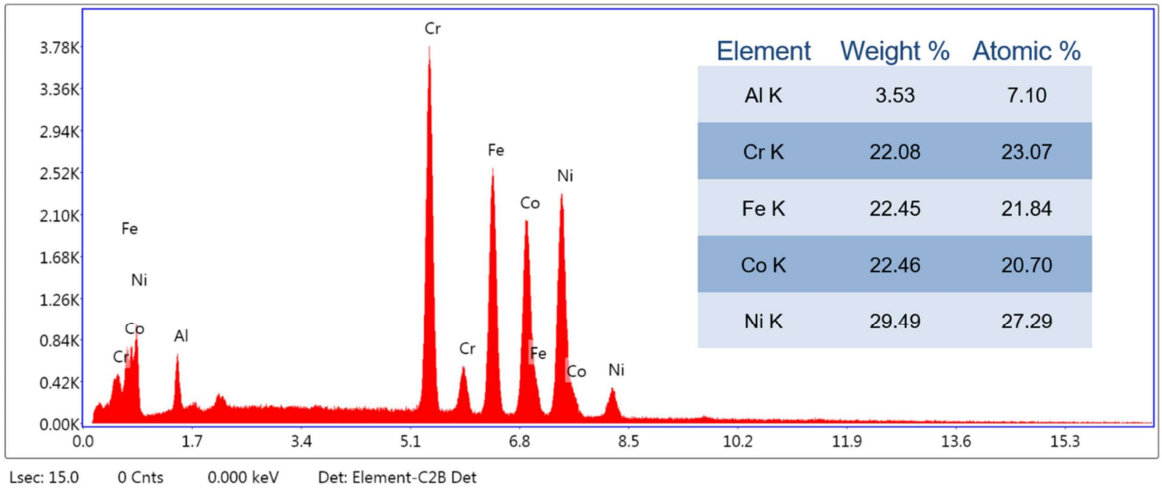

Element	Weight %	Atomic %
Al K	3.53	7.10
Cr K	22.08	23.07
Fe K	22.45	21.84
Co K	22.46	20.70
Ni K	29.49	27.29

Fig. 4. EDS results of point "B" in Fig. 2.

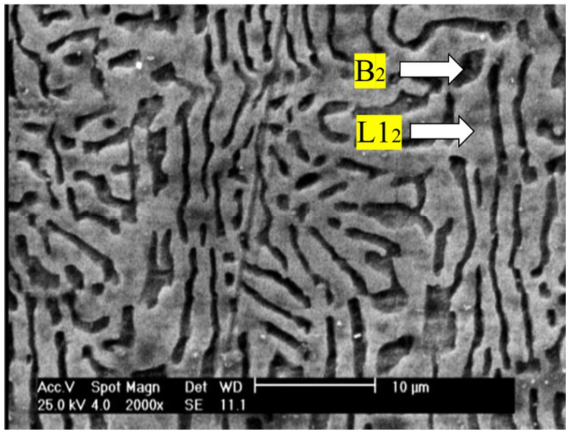

Fig. 5. Phases $L1_2$ and B_2 in the homogenized specimen.

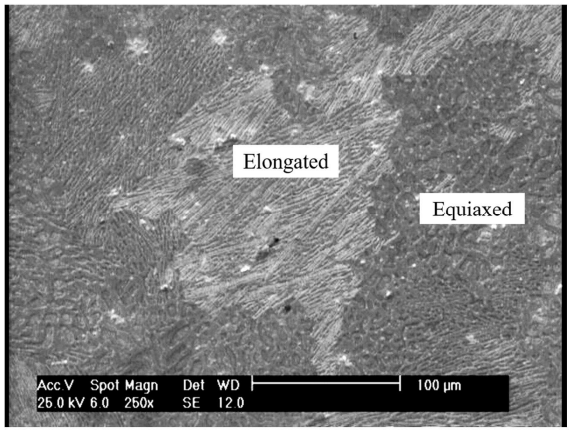

Fig. 6. SEM micrograph of cold-rolled and annealed specimen.

This shows that recrystallization has happened during the annealing. With the growth of recrystallized grains, a part of energy stored during cold rolling has been released due to annealing; but the specimen has not been fully annealed and partial annealing took place in this case. Hence, the equiaxed phases/grains are visible next to the elongated phases/grains formed due to cold work [14, 22, 23].

3.2. Hardness

According to Table 3, the minimum amount of hardness belongs to the homogenized sample and the hardness of the cold-rolled followed by anneal specimens is between those of as-cast and homogenized specimens. The lower amount of hardness in the homogenized specimen is due to the increase in the percentage of $L1_2$ soft phase during the homogenization.

Table 3. Micro- and macro-hardness of as-cast, homogenized, cold-rolled and annealed samples

Sample	Micro-hardness (HV)	Macro-hardness (HRC)
As-cast	375±7	37±1
Homogenized	243±5	23±1
Cold-rolled and annealed	318±6	33±1

Due to the presence of both elongated and equiaxed structures in the cold-rolled and annealed samples, the hardness of this specimen is between the hardness of as-cast and homogenized cases.

3.3. Shear properties

Fig. 7 shows the SPT curves for the as cast, homogenized, cold-rolled and annealed specimens in which the shear stress versus normalized displacement is plotted. According to Fig. 7 and Table 4, the minimum amount of both yield and ultimate shear strength belongs to the homogenized specimen because of its exposure to high temperatures for a long period and the subsequent growth of FCC phases. The yield and ultimate shear strength of the cold-rolled and annealed specimen is between those of as-cast and homogenized specimens due to the presence of a mixture of elongated and equiaxed phases/grains next to each other. The higher strength of the as-cast specimen compared to that of the homogenized and cold-rolled followed by annealing specimens is due to the residual stresses of the casting

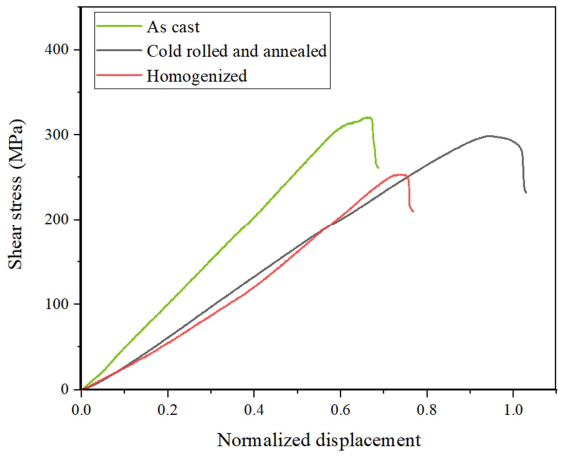

Fig. 7. Shear punch testing curves of as-cast, homogenized, cold-rolled and annealed specimens.

Table 4. Shear properties of as-cast, homogenized, cold-rolled and annealed specimens

Sample	Yield stress (MPa)	Ultimate shear stress (MPa)
As-cast	282±9	311±10
Homogenized	226±7	248±8
Cold-rolled and annealed	255±8	304±9

process, the presence of Cr-rich precipitates and the lower percentage of phase $L1_2$ in its microstructure.

4. Conclusion

- The as-cast AlCoCrFeNi$_{2.1}$ high-entropy alloy has a eutectic lamellar structure containing FCC/$L1_2$ phase and the BCC/B_2 phase. In the homogenized specimens, the percentage of $L1_2$ phase is higher than that of the as-cast case.
- The cold-rolled and annealed structure consists of a combination of elongated and equiaxed phases/grains.
- The homogenized specimen has the minimum amounts of hardness and yields/ultimate shear strength. This can be due to the grain growth as well as the formation of $L1_2$ phases during homogenization.
- The highest yield/ultimate shear strength and hardness belong to the as-cast specimen due to the residual stresses of the casting process, the presence of Cr-rich precipitates and the lower percentage of phase $L1_2$ in its microstructure.
- The hardness and yield/ultimate shear strength of the cold-rolled and annealed samples is between that of as-cast and homogenized specimens due to the presence of a mixture of elongated phases/grains along with the almost equiaxed phases/grains.

5. References

[1] S.S. Nene, K. Liu, M. Frank, R.S. Mishra, R.E. Brennan, K.C. Cho, Z. Li, D. Raabe, Enhanced strength and ductility in a friction stir processing engineered dual phase high entropy alloy, *Scientific reports*, 7(1) (2017) 1-7.

[2] D. Choudhuri, S. Shukla, P. Jannotti, S. Muskeri, S. Mukherjee, J. Lloyd and R.S. Mishra, Characterization of as-cast microstructural heterogeneities and damage mechanisms in eutectic AlCoCrFeNi2.1 high entropy alloy, *Materials Characterization*, 158 (2019) 109955.

[3] Y. Wang, W. Chen, J. Zhang, J. Zhou, A quantitative understanding on the mechanical behavior of AlCoCrFeNi2.1 eutectic high-entropy alloy, *Journal of Alloys and Compounds*, 850 (2021) 156610.

[4] E. Abbasi, K. Dehghani, Phase prediction and microstructure of centrifugally cast non-equiatomic Co-Cr-Fe-Mn-Ni (Nb, C) high entropy alloys, *Journal of Alloys and Compounds*, 783 (2019) 292-299.

[5] M.H. Asoushe, A.Z. Hanzaki, H.R. Abedi, B. Mirshekari, T. Wegener, S.V. Sajadifar and T. Niendorf, Thermal stability, microstructure and texture evolution of thermomechanical processed AlCoCrFeNi2.1 eutectic high entropy alloy, *Materials Science and Engineering: A*, 799 (2021) 140012.

[6] F. Otto, Y. Yang, H. Bei, E.P. George, Relative effects of enthalpy and entropy on the phase stability of equiatomic high-entropy alloys, *Acta Materialia*, 61(7) (2013) 2628-2638.

[7] O. N. Senkov, G.B. Wilks, D.B. Miracle, C.P. Chuang, P.K. Liaw, Refractory high-entropy alloys, *Intermetallics*, 18(9) (2010) 1758-1765.

[8] M.H. Tsai, J.W. Yeh, High-entropy elloys: a critical review, *Materials Research Letters*, 2(3) (2014) 107-123.

[9] A.V. Kuznetsov, D.G. Shaysultanov, N.D. Stepanov, G.A. Salishchev, O.N. Senkov, Tensile properties of an AlCrCuNiFeCo high-entropy alloy in as-cast and wrought conditions, *Materials Science and Engineering: A*, 533 (2012) 107-118.

[10] Y. Zhang, X. Wang, J. Li, Y. Huang, Y. Lu, X. Sun, Deformation mechanism during high-temperature tensile test in an eutectic high-entropy alloy AlCoCrFeNi2.1, *Materials Science and Engineering: A*, 724 (2018) 148-155.

[11] Y. Lu, Y. Dong, S. Guo, L. Jiang, H. Kang, T. Wang, B. Wen, Z. Wang, J. Jei, Z. Cao, H. Ruan, T. Li, A promising new class of high-temperature alloys: eutectic high-entropy alloys, *Scientific reports*, 4(1) (2014) 1-5.

[12] X. Jin, Y. Zhou, L. Zhang, X. Du, B. Li, A novel Fe20Co20Ni41Al19 eutectic high entropy alloy with excellent tensile properties, *Materials Letters*, 216 (2018) 144-146.

[13] X. Chen, J.Q. Qi, Y.W. Sui, Y.Z. He, F.X. Wei, Q.K. Meng, Z. Sun, Effects of aluminum on microstructure and compressive properties of Al-Cr-Fe-Ni eutectic multi-component alloys, *Materials Science and Engineering: A*, 681 (2017) 25-31.

[14] I. Wani, T. Bhattacharjee, S. Sheikh, Y. Lu, S. Chatterjee, S. Guo, Effect of severe cold-rolling and annealing on microstructure and mechanical properties of AlCoCrFeNi2.1 eutectic high entropy alloy, *IOP Conference Series: Materials Science and Engineering*, 194(1) (2017) 012018.

[15] A. Lozinko, R. Gholizadeh, Y. Zhang, U. Klement, N. Tsuji, O. Mishin, Evolution of microstructure and mechanical properties during annealing of heavily rolled AlCoCrFeNi2.1 eutectic high-entropy alloy, *Materials Science and Engineering: A*, 833 (2022) 142558.

[16] E. Abbasi, K. Dehghani, Effect of Nb-C addition on the microstructure and mechanical properties of CoCrFeMnNi high entropy alloys during homogenisation, *Materials Science and Engineering: A*, 753 (2019) 224-231.

[17] E. Abbasi, K. Dehghani, Microstructure and mechanical properties of Co19Cr20Fe20Mn21Ni19 and Co19Cr20Fe20Mn21Ni19Nb0.06C0.8 high-entropy/compositionally-complex alloys after annealing, *Materials Science and Engineering: A*, 772 (2020) 138812.

[18] E. Lucon, J.T. Benzing, N. Derimow, N. Hrabe, Small punch testing to estimate the tensile and fracture properties of additively manufactured Ti-6Al-4V, *Journal of Materials Engineering and Performance*, 30(7) (2021) 5039-5049.

[19] R.K. Guduru, K.A. Darling, R. Kishore, R.O. Scattergood, C.C. Koch, K.L. Murty, Evaluation of mechanical properties using shear–punch testing, *Materials Science and Engineering: A*, 395(1-2) (2005) 307-314.

[20] X. Gao, Y. Lu, B. Zhang, N. Liang, G. Wu, G. Sha, J. Liu, Y. Zhao, Microstructural origins of high strength and high ductility in an AlCoCrFeNi2.1 eutectic high-entropy alloy, *Acta Materialia*, 141 (2017) 59-66.

[21] I.S. Wani, T. Bhattacharjee, S. Sheikh, P.P. Bhattacharjee, S. Guo, N. Tsuji, Tailoring nanostructures and mechanical properties of AlCoCrFeNi2.1 eutectic high entropy alloy using thermo-mechanical processing, *Materials Science and Engineering: A*, 675 (2016) 99-109.

[22] I.S. Wani, T. Bhattacharjee, S. Sheikh, I.T. Clark, M.H. Park, T. Okawa, Cold-rolling and recrystallization textures of a nano-lamellar AlCoCrFeNi2.1 eutectic high entropy alloy, *Intermetallics*, 84 (2017) 42-51.

[23] S.R. Reddy, U. Sunkari, A. Lozinko, S. Guo, P.P. Bhattacharjee, Development and homogeneity of microstructure and texture in a lamellar AlCoCrFeNi2.1 eutectic high-entropy alloy severely strained in the warm-deformation regime, *Journal of Materials Research*, 34(5) (2019) 687-699.